S1 Downhole logging

Initially, it was intended to use the memory sondes in their authentic autonomous operation mode, where the sonde is dropped into a drill pipe, landing at the drill bit, and measuring while being pulled up along with the drill pipe. The very special Hipercorig drilling design without a drill pipe reaching from the lake floor to the drilling barge, did not easily allow this typical logging-while-tripping method of memory sondes. A special technical adaption needs to be made for a future actual memory mode use of the sondes. Therefore, the data acquisition was performed in wireline mode. Unfavorably, a regular wireline logging was not possible because there is no pipe between drilling barge and the lake floor to guide logging sondes to the borehole mouth. Instead, the logging sondes had to be guided with the ropes originally used to guide the Hipercorig piston corer. The difficulties mentioned, including the synchronization of the pulling, due to the special set up, could not have happened when using the true memory mode logging-while-tripping method. The available logging time window of one day shift did not allow a second logging run.

S2 Composite profile

The composite profile was created using the established methods of the IODP drilling (e.g. Hall et al., 2017), creating tables for: (i) splice, (ii) tie-points and (iii) vertical offset (see *Table S1, S2* and *S3*) and visualized through the software of (Ortler, 2023).

The "Core depth below lake floor" (CLF-A) scale describes the depth below lake floor, below the mudline of both drilled holes during the H^3 coring campaign. Gas expansion, water loss or relief of overburden may lead to a change of the sedimentary features within the coring positions. Hence, drilling effects and core expansion can cause stratigraphically unreasonable overlaps. In theory, the composite depth scale, below overcomes and corrects such artifacts.

The "Core composite depth below lake floor" (CCLF-A) scale includes the identified coeval, laterally continuous intervals in the drilled holes (which usually occur at different CLF-A scales in each hole). The construction of the CCLF-A scale, offsetting the individual cores with a constant amount without stretching or squeezing core segments. This will create a vertical depth offset for every core section, which can be linked to the CCLF-A scale. If a core gap is aligned, the subsequent core sections can still be tied to another, but need they are "floating" on the CCLF-A scale and need to be denoted as "APPENDED".

The "Splice core composite depth below lake floor" (CCSF-D) scale refers to a subset of the CCLF-A scale which is a complete stratigraphic section (splice), constructed using the previously established tie points. Intervals which are not included in the primary splice (CCLF-D) maintain the CCLF-A scale. In case of core gaps, any splice sections below a gap is appended to those above, and described as floating splice section.

For the events E2 and E3, only the borehole B was used (hence 'floating' sections) to be able to correlate the signal better to the borehole logging, which was conducted at borehole B. Both drilled holes show slight differences, such as E3 within hole A showing more deformation structures, compared to the hole B drilled more in the east and south, which shows a coarser basal E2 deposit.

Overall, the composite profile correlates very well with *the HAS_2016-1 core* (Lauterbach et al., 2023) and can be improved at least at two intervals (CL3 to CL4 and CL7 to CL8), as well as the water to sediment interface with integrating *HAS_2016-1* into the splice. For now, the H^3 composite core was only anchored to *HAS_2016-1* with CL1.

Table S1: Composite depth-splice for the sediments from Lake Hallstatt (Salzkammergut, Austria); see separate file for Table.

Table S2: Tie-points for the sediments from Lake Hallstatt (Salzkammergut, Austria), see separate file for Table

Table S3: Vertical offset for the sediments from Lake Hallstatt (Salzkammergut, Austria), see separate file for Table

S2.1 Correlation lines (CL, tie points)

The correlation lines include tie points and appended core sections (see Table S2). Correlation lines with the highest confidence are traditional tie points, identified coeval, laterally continuous intervals in the drilled holes. Whereas correlation lines with intermediate and low confidence describe appended core sections. The intermediate confidence is likely able to be tied, with further analysis while low confidence correlation lines may still be appended.

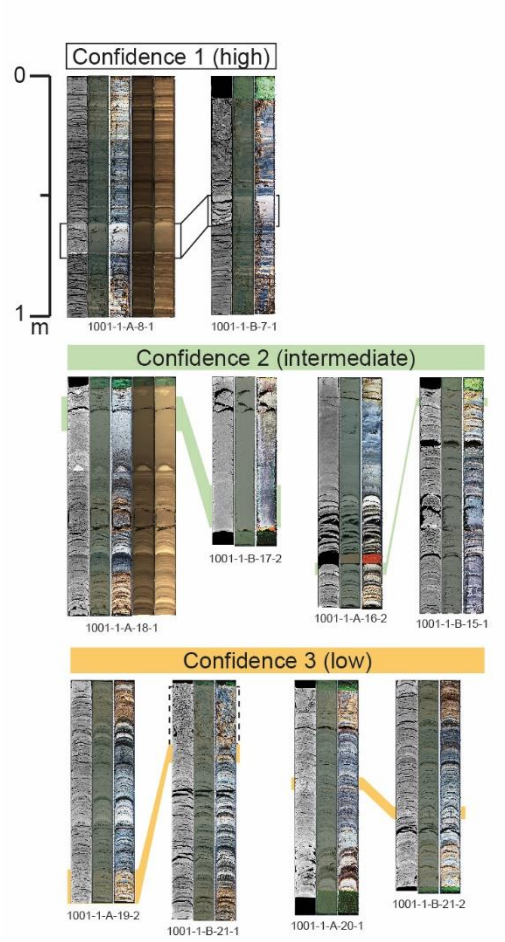

Figure S1: Confidence level of the correlation lines of the composite core from Lake Hallstatt (Salzkammergut, Austria); Confidence 1: tie point of coeval identified intervals; Confidence 2: appended core section, which likely will be tied with additional analyses; Confidence 3: appended core section, with low confidence, which need additional analyses to be tied.

S3 Data handling and processing

A pipeline structure through Python is set up to visualize the borehole logging data and to separate and visualize the MSCL whole round processed data (density and magnetic susceptibility) using *pandas* (McKinney, 2010), *NumPy* (Harris et al., 2020) and *Matplotlib* (Hunter, 2007). In combination with the splice table of the composite profile (see Table S1), the resulting splice is plotted in three ways: (i) processed raw data (ii) outlier filtered data (iii) Gaussian smoothed data (15-points). Also, an additional correction of the magnetic susceptibility data was needed for the following core sections (1001-1-B-3-1, 1001-1-B-3-2, 1001-1-B-4-1, 1001-1-B-4-2, 1001-1-B-5-1, 1001-1-B-5-2, 1001-1-B-6-1, 1001-1-B-6-2 and 1001-1-B-12-1, 1001-1-B-12-2). The scanned cores showed a MS sensor drift due to partly scanning of the initial calibration piece. The average value of the calibration piece should represent 0, which was afterwards ~14. Therefore, 14 was subtracted from the above-mentioned cores.

S4 Seismic facies

Table S4: Overview of seismic facies and expected lithology of Lake Hallstatt (Salzkammergut, Austria).

Facies ID	Seismic facies	Description	Expected lithology
F1	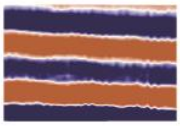	Parallel, high-amplitude continuous horizontal reflections	Lacustrine sedimentation (sand to clay)
F2	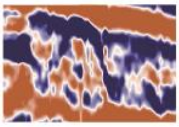	semi-transparent and non-continuous reflections with variable amplitudes and hummocky-to-deformed geometries	Mostly sand and deformed mud, with coarse material at base
F3	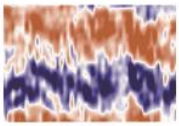	diffuse low-amplitude reflections	Compacted lacustrine sedimentation (sand to clay)
F4	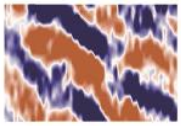	moderate amplitudes, with interlayered chaotic facies	Lacustrine sedimentation (sand to clay), with intercalated turbidites
F5	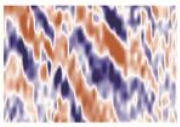	medium-amplitude reflections	Compacted lacustrine sedimentation (sand to clay)

S5 Coring disturbance and difficulties

The various coring disturbances are mainly present in the upper 15 m and mainly in the upper section of the 2 m core. Here, it can be up to 30 cm in the first core section, which are affected by coring disturbance and imprints of the piston. This decreases within the deeper coring sections. Furthermore, coring difficulties occurred in borehole A and B at ~25 m coring depth, and in borehole A below 38 m, as well as in borehole B also at ~38 m coring depth, possible related to coarse (sandy to pebble) material. The coring difficulties coincide with the CL difficulties. Here, additional flushing of the casing was needed, which resulted in additional sediment on top of the normal stratigraphy, which was cored. The flushing potentially also eroded some of the very top parts of the next section.

S6 Age-depth modelling

The current age model using Bacon v3.0.0 software package for R (Blaauw and Christen, 2011) was run with a suggested 2 cm accumulation rate, 136 sections of 30 cm sections for a composite core length of 55 m. The standard memory strength of 10 and mean of 0.5 were used, as well as 15 000 iterations set to run. In total four hiatuses were set below each major MTD, with a maximum hiatus of 2 000 years. Furthermore, the maximum age of the age model was set to 15 000 years. The anchored topmost sediment of H^3 was used as starting point. From the correlation to the *HAS_2016-1* core, the year 1975 was used as starting age with an error of 10 years. We observed six subunits for the Holocene unit, with various lamination thicknesses. The observed lithological changes indicate multiple accumulation rates. The created age model only uses the suggested 2 cm accumulation rate for the background sedimentation. Hence, the spiky iteration and memory output supports that various accumulation rates need to be considered. Individual age-depth model runs with set boundary (change of accumulation rate) will allow a better age constraint, in combination with additional ages in the future.

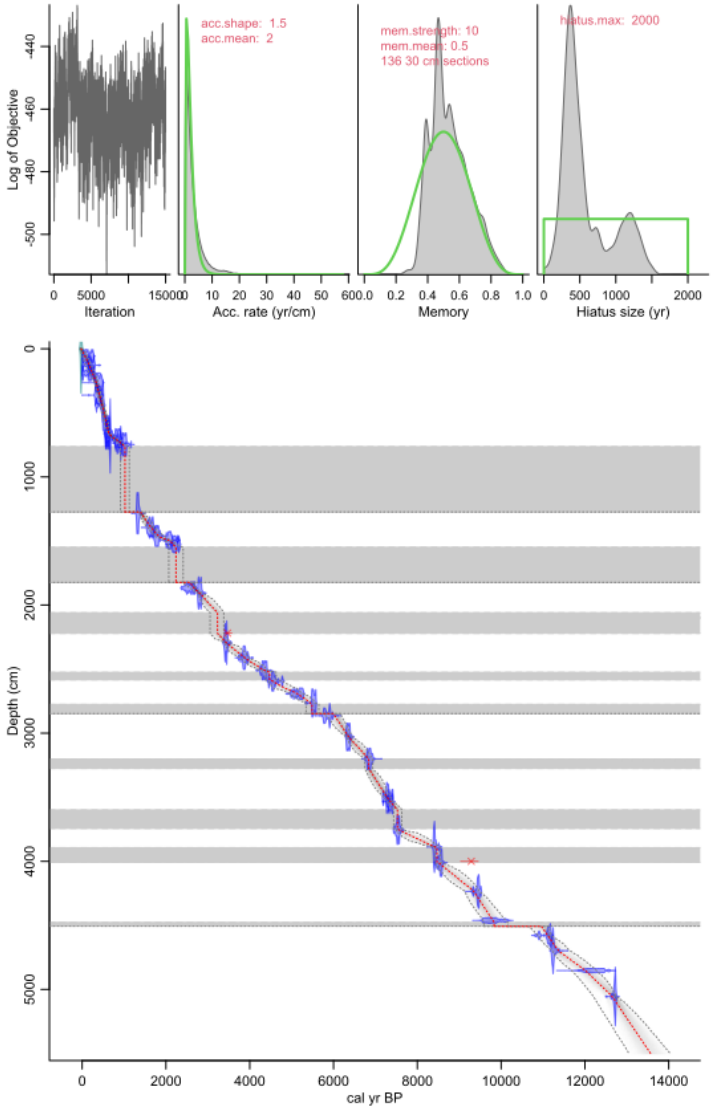

Figure S2: Age-depth model output from Bacon v3.0.0 for the composite core from Lake Hallstatt (Salzkammergut, Austria) with 22 (this study) radiocarbon dates (^{14}C), 2 omitted radiocarbon (^{14}C) dates (in red) and 17 projected ^{14}C dates from Lauterbach et al. (2023).

Table S5: Tie-points to project the ^{14}C ages of the *HAS_2016-1* core (Lauterbach et al., 2023) to the H^3 composite profile from Lake Hallstatt (Salzkammergut, Austria)

Tie-point Nr	HAS_2016-1 AMS ^{14}C dates lab code name	HAS_2016-1 Master composite depth [m]	H^3 composite depth [m]	H^3 core name	H^3 section depth [m]
1	Poz-87261	0.5425	0.575	1001-1-A-1-1	0.48
2	Poz-87262	2.19	1.285	1001-1-B-1-1	0.28
3	Poz-87263	2.74	1.895	1001-1-B-1-1	0.89
4	Poz-87307	3.47	2.65	1001-1-B-1-2	0.65
5	Poz-87308	3.955	3.62	1001-1-A-2-2	0.1
6	Poz-87309	4.68	4.415	1001-1-B-2-1	0.75
7	Poz-87313	6.21	6.425	1001-1-A-3-2	0.59
8	Poz-87314	6.395	6.62	1001-1-A-3-2	0.785
9	Poz-95546	6.545	6.805	1001-1-B-3-1	0.64
10	Poz-87315	6.76	6.995	1001-1-B-3-1	0.83
11	Poz-87316	7.3	7.375	1001-1-B-3-2	0.22
12	Poz-87317	7.4	7.475	1001-1-B-3-2	0.32
13	Poz-87319	8.67	12.836	1001-1-B-6-1	0.56
14	Poz-87321	9.71	13.951	1001-1-B-6-2	0.68
15	Poz-87323	10.3925	14.606	1001-1-A-8-2	0.245
16	Poz-95545	10.73	14.946	1001-1-A-8-2	0.585
17	Poz-87325	11.0325	15.256	1001-1-B-7-1	0.77

Table S6: Overview table of event deposits, clastic unit and main coring gaps for the sediments from Lake Hallstatt (Salzkammergut, Austria).

Name	Section depth		CCLF-A		Thickness [m]
	Top [cm]	Bottom [cm]	Top [m]	Bottom [m]	
Clastic unit	40	71	2.4	6.875	4.475
E2	48.5	46	7.64	12.736	5.096
E2 Turbidite Hole B	48.5	48	7.64	9.121	1.481
E2 Sand/Organic Hole B	48	78	9.121	9.421	0.3
E2 MTD Hole B	78	46	9.421	12.736	3.315
E3 Turbidite Hole B	2	84.5	15.496	17.296	1.8
E3 Sand/Organic Hole B	84.5	43.5	17.296	17.755	0.459
E3 MTD Hole B	43.5	87.5	17.755	18.195	0.44
E4	98.5	37.5	20.606	20.991	0.385
E5	37.5	69	20.991	22.206	1.215
E6	32.5	91	25.251	25.836	0.585
E7	25.5	97	27.756	28.471	0.715
main coring gap	8		28.471		
E8	75	49.5	32.021	32.761	0.74
E9	55	40	35.996	37.436	1.44

E10	22	47.5	38.936	40.08	1.14
E11	89.5	120.5	44.766	45.08	0.31

S7 Core-Log-Seismic-Integration

The borehole logging (performed within hole B) is tied to the composite core profile of hole A and B based on the magnetic susceptibly (MS) data (see Table S7). The confidence level of each logging tie-point (LTP) ranges from 1 to 3 (high confidence to low confidence). The overall trend of both datasets are in agreement with each other. Nevertheless, some differences are observed such as the evolution of the core logged MS data (Fig. 6) of E2 and E3 compared to the borehole logging data (see also *Sect. 5.2*). As described in *Sect. S2*, only core segments of hole B were appended for those two deposits. The base of E2 is clearly defined in both data sets within a downhole increasing MS trend (between tie points T6 and T7), yet the MS trends within E2 are different: the respective sediment core sections are dominated by a mass-transport deposit (of a carbonate rich facies) with low amplitude MS values at the base, and followed by spiky, higher amplitude MS values in the overlying organic rich interval containing sand. In contrast the borehole logging MS data, shows a gradual decrease of MS values from the base to the top of the deposit. The missing of the high amplitude values within the borehole logging data may be due to the lower vertical resolution of the borehole logging sensor and the different trend within the sediment core may also be influenced by small scale (i.e. within the MSLC logged whole round core) differences of organic material and carbonate rich facies, influencing the MS loop sensor of the MSCL. Likewise, the evolution of E3 shows higher MS values at LTP 10, with a decreasing trend of MS values towards the top within the borehole logging data, and stable to a slight increase of MS values in the sediment core data.

Table S7: Logging tie-points of MS borehole logging (Hole B) and MS core logging (composite profile) data for Lake Hallstatt (Salzkammergut, Austria).

Logging tie points Nr [LTP]	MS borehole logging of Hole B [m]	MS sediment core of composite profile [m]	Tie point description	confidence level of correlation (1-3 high-low)
1	127.26	3.07	Small positive MS peak on top of ~1.5m-thick interval characterized by a general increasing-upward trend	1
2	129.46	4.68	Lowest value followed by an increasing trend (with two lower values within the borehole logging data)	2
3	130.96	7.18	Lowest value below a increasing-upward trend and negative peak in borehole logging and core logging data, respectively	2
4	133.06	9.61	A peak of high values on top of lower values, followed by a decreasing trend	3
5	133.86	10.38	Lowest value on top of an interval with higher values	2
6	135.16	12.28	Lowest value on top of a general higher amplitude of MS values and followed with lower amplitude values	1
7	136.06	13.45	Highest peak of high amplitude MS values followed with a decrease in MS amplitude	1
8	137.66	15.31	Small positive peak on top of an general increasing upward MS trend	2
9	139.56	16.51	Low values of MS on top of higher MS values, followed by an generally increasing upward MS trend	3
10	140.06	17.67	Small positive MS peak on top of an decreasing trend of low amplitude,	3

			followed by an interval of ~2m stable MS values	
11	141.16	19.37	MS peak on top of a decreasing trend of MS values, followed by an interval of similar amplitude	2
12	142.16	20.34	Positive MS peak on top of a short MS low, followed by a decrease in MS amplitude	1
13	143.06	21.34	MS peak on top of a stable MS interval of ~1m followed by a step wise decrease/stable interval (borehole/sediment)	2
14	144.26	22.84	Dominant MS peak on top of a prominent MS low, followed by a step wise MS decrease	1
15	144.96	23.57	Dominant MS peak on top of low MS values followed by a prominent MS low	1
16	146.96	26.04	MS peak on top of an MS increase followed by a decrease over ~2m	2
17	148.26	26.73	Prominent MS peak in borehole logging on top of stable MS interval, MS peak in core logging on top of a MS low and followed by a ~1m interval of increased MS values	3
18	150.36	28.80	Dominant high MS peak followed by a decrease in MS amplitude	1
19	151.06	29.46	High MS peak on top of the increased MS amplitude interval, followed by a small decrease of MS values	2
20	157.36	36.12	High MS peak on top of general low MS values, followed by an increase in MS amplitude	2
21	158.76	37.48	Small positive MS peak on top of an ~1m interval of low MS values, followed by more stable MS values	2
22	159.86	38.48	Positive MS peak on top of stable MS interval, followed by a decrease of MS values	2
23	162.06	40.10	Dominant high MS peak followed by general stable interval of ~1m	1
24	162.56	41.03	High MS peak on top of generally low MS values, followed by a dominant MS peak	1
25	163.86	42.29	High MS peak on top of generally low MS values	2
26	164.76	43.90	High MS peak on top of generally low MS values	2
27	166.46	45.39	Small MS peak on top of decreased MS values and followed by decreasing/stable MS values (borehole/sediment respectively)	3
28	167.76	47.44	MS peak on top of a low MS values, followed by a general trend towards lower MS values (with the exception of a dominant peak within the core logging MS data)	3
29	168.76	48.37	MS double peak in borehole logging data, and broad MS peak in core logging on top of lower MS values	3

30	169.86	50.07	High MS peak in both datasets on top of a steep increase of MS values, followed with lower values	2
31	170.86	51.21	MS peak in-between two low MS intervals	3
32	171.36	52.01	Positive MS peak on top of generally low MS values	2
33	173.06	53.92	Low MS value on top of an increasing trend, and followed by low MS values	3

References

Blaauw, M. and Christen, J. A.: Flexible paleoclimate age-depth models using an autoregressive gamma process, Bayesian Anal., 6 (3), 457–474, https://doi.org/10.1214/11-BA618, 2011.

Hall, I., Hemming, S., LeVay, L., Barker, S., Berke, M., Brentegani, L., Caley, T., Cartagena-Sierra, A., Charles, C., Coenen, J., and others: Expedition 361 methods, in: Proceedings of the International Ocean Discovery Program, 361, International Ocean Discovery Program, 2017.

Harris, C. R., Millman, K. J., van der Walt, S. J., Gommers, R., Virtanen, P., Cournapeau, D., Wieser, E., Taylor, J., Berg, S., Smith, N. J., Kern, R., Picus, M., Hoyer, S., van Kerkwijk, M. H., Brett, M., Haldane, A., del Río, J. F., Wiebe, M., Peterson, P., Gérard-Marchant, P., Sheppard, K., Reddy, T., Weckesser, W., Abbasi, H., Gohlke, C., and Oliphant, T. E.: Array programming with NumPy, Nature, 585, 357–362, https://doi.org/10.1038/s41586-020-2649-2, 2020.

Hunter, J. D.: Matplotlib: A 2D Graphics Environment, Comput. Sci. Eng., 9, 90–95, https://doi.org/10.1109/MCSE.2007.55, 2007.

Lauterbach, S., Strasser, M., Kowarik, K., Reschreiter, H., Mandl, G. W., Spötl, C., Plessen, B., and Brauer, A.: Large-scale mass movements recorded in the sediments of Lake Hallstatt (Austria)–evidence for recurrent natural hazards at a UNESCO World Heritage site, J. Quaternary Science, 38 (2), 258–275, https://doi.org/10.1002/jqs.3472, 2023.

McKinney, W.: Data Structures for Statistical Computing in Python, Python in Science Conference, Austin, Texas, 56–61, https://doi.org/10.25080/Majora-92bf1922-00a, 2010.

Ortler, M.: Marcel1415/splice: v0.2-alpha, , https://doi.org/10.5281/zenodo.7966002, 2023.